Stability of vorticity defects in viscous shear

By N E I L J. B A L M F O R T H

Department of Theoretical Mechanics, University of Nottingham, Nottingham, NG7 2RD, UK

The stability of viscous shear is studied for flows that consist of predominantly linear shear, but contain localized regions over which the vorticity varies rapidly. Matched asymptotic expansion simplifies the governing equations for the dynamics of such 'vorticity defects'. The normal modes satisfy explicit dispersion relations. Nyquist methods are used to find and classify the possible instabilities. The defect equations are analysed in the inviscid limit to establish the connection with inviscid theory. Finally, the defect approximation is used to study nonlinear stability using weakly nonlinear techniques, and the initial value problem using Laplace transforms.

1. Introduction

The stability of a shearing fluid at high Reynolds number is often determined by solving for its normal modes. Given those modes, one can then determine something of the finite-amplitude behaviour using weakly nonlinear expansion. The normal mode problem, for two-dimensional incompressible fluid, is the Orr–Sommerfeld equation, an equation that is difficult to solve when the viscosity becomes small (Drazin & Reid 1981). As a result, general features of the stability properties of viscous shears are not well understood, such as the passage to the inviscid limit and the dependence on the velocity profile.

The purpose of the present paper is to attack the viscous shear flow problem from a novel direction. The study focuses on the stability of particular types of shear flow. These flows consist of predominantly linear shear. However, seeded within this ambient shear is a localized region over which the vorticity deviates from the uniform and varies rapidly (though it is fixed in the direction of the flow). To the bulk of the flow, the localized region appears to be a velocity jump given by the integral vorticity contained inside the region; for this reason, that region is referred to as a 'vorticity defect'. An example is displayed in figure 1. In a viscous fluid, such a basic state must be maintained by a body force on the fluid, which we assume to result from some additional physical effect.

Such states were first considered by Gill (1965), who was primarily interested in inviscid stability. In that context, the defect provides an order-one vorticity gradient that is sufficient to destabilize the flow. Gill's vision of the defect was as a model of the wake of a solid cylinder in a shear flow, over times short enough that viscosity was negligible. Defects, however, may approximately model some astrophysical and geophysical flows, and might be realized in laboratory settings.

For flows with defects, the equations governing the vorticity within the defect can be simplified using matched asymptotic expansion. For inviscid defects, the expansion leads to a linear theory of a particularly clear and concise form (Gill 1965; Balmforth, del Castillo-Negrete & Young 1996, hereafter referred to as paper I). The aim of the
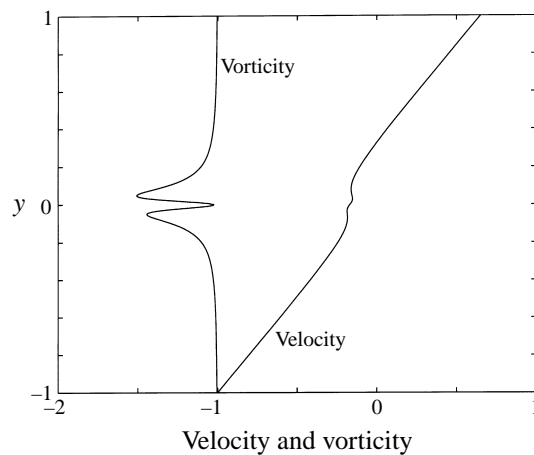
FIGURE 1. A vorticity defect in Couette flow (shown for the profile (5.1), with $\epsilon = 0.05$, $\alpha = 5$, $\beta = 50$ and $f = 1$).

current study is a complementary discussion of the viscous problem. In fact, 'defect theory' provides an approximate, simplified description that hopefully captures the essential mathematical and physical details of the problem.

Admittedly, the special form of profiles like that shown in figure 1 detracts from the generality of the results. However, the shape of the mean defect is completely arbitrary. Moreover, more complicated profiles can be seeded with vorticity defects (paper I). Even so, there is no guarantee that the defect problem captures the dominant physics of the entire flow. None the less, the simplifications afforded by the reduction of the problem makes the theory interesting and useful as a framework in which to study shear flow dynamics.

The defect theory is summarized in §2. The linear stability analysis is described first for the inviscid problem in §3, then for viscous defects in §§4–5. In contrast to the Orr–Sommerfeld problem, the linear stability problem for defects can be reduced to a dispersion relation involving a single integral. These relations allow one to use Nyquist methods to find unstable modes, and remove the need for complicated numerical calculations. Previously, such dispersion relations have only been available for long wave expansions (Howard 1959) and profiles with piecewise-constant vorticity whose physical significance is questionable for viscous flow (Drazin 1961).

A key feature of defect theory is that with it one can pass relatively easily to the inviscid limit, thence explore how the viscous problem limits to the inviscid one. This limit is important to understand in order to verify the applicability of inviscid theory, particularly in the circumstance that viscosity destabilizes the shear flow. The inviscid limit is explored in §6.

Finally, though normal mode analysis uncovers the existence of instability, it does not always provide a complete picture of the evolution of the flow. In particular, it is often conjectured that shear flow instability is *subcritical*; that is, that finite-amplitude time-dependent motions can be triggered at lower Reynolds numbers by sufficiently large disturbances. Some idea of such possibilities is provided by weakly nonlinear theory (Stuart 1960). For defects, weakly nonlinear analysis is relatively straighforward (Appendix B). Also, the utility of the whole normal mode approach has recently been brought into question over the importance of transient amplification (Schmid *et al.* 1993). Such effects are rather indirectly described by the normal modes.

In fact, for infinite or inviscid shears these effects are a property of a continuous spectrum rather than discrete modes. One way around this shortcoming of the normal mode approach is to solve the initial-value problem directly with Laplace transforms. A brief discussion of these two topics constitutes §7, and some concluding remarks are given in §8.

2. Defect formulation

The details of the matched asymptotic expansion are given in paper I; this expansion is somewhat related to the methods of Stewartson (1978) and Warn & Warn (1978) used to study the forced Rossby wave critical layer problem. The problem concerns a shear flow of a two-dimensional incompressible fluid in a channel, $-\infty < x < \infty$ and $-1 \leqslant y \leqslant 1$. The flow is predominantly a linear shear flow, but is mildly forced in a narrow region of size ϵ, the defect, which is located (for convenience) along the central line of the channel, $y = 0$.

With suitable scalings for length and time, the velocity components can be expressed in terms of a dimensionless streamfunction,

$$\Psi(x, y, t) = \tfrac{1}{2}(y^2 - 1) + \epsilon^2 \psi(x, y, t), \tag{2.1}$$

composed of the Couette background, $(y^2 - 1)/2$, and a term containing all departures from that flow, $\epsilon^2 \psi$. The scaling of these departures implies that the vorticity of the defect itself is order ϵ. The associated vorticity gradient, however, is order one and therefore critical to instability (Gill 1965).

The expansion begins from the dimensionless vorticity equation,

$$\epsilon \omega_t + y \omega_x + \epsilon^2 \frac{\partial(\psi, \omega)}{\partial(x, y)} = \epsilon^3 \nu \nabla^2 \omega + \text{forcing terms}, \tag{2.2}$$

where the vorticity, ω, and streamfunction, ψ, are related by

$$\omega = \nabla^2 \psi, \tag{2.3}$$

and ν is the dimensionless coefficient of viscosity, scaled such that the Reynolds number is order ϵ^{-3}, in which case viscous effects are felt primarily within the defect.

Next one finds a solution valid in the 'outer' part of the flow (that is, the bulk of the fluid outside the defect), and matches to an 'inner' solution appropriate inside the defect. The salient result is a reduced equation for the defect's vorticity, $\mathscr{Z}(x, \eta, t)$, where $\eta = y/\epsilon$ is an inner, or defect, coordinate:

$$\mathscr{Z}_t + \eta \mathscr{Z}_x + \mathscr{Z}_\eta B_x = \nu \mathscr{Z}_{\eta\eta} + \text{forcing terms}, \tag{2.4}$$

in which $B(x, t)$ is the leading-order piece of the streamfunction which is constant inside the defect, and its Fourier transform in x is given by

$$\hat{B}(k, t) = -\frac{\tanh k}{2k} \int_{-\infty}^{\infty} \hat{\mathscr{Z}}(k, \eta, t) \, \mathrm{d}\eta. \tag{2.5}$$

The boundary conditions imposed on (2.4) are that $\mathscr{Z} \to O(\eta^{-2})$ as $\eta \to \pm\infty$. For future use, let

$$\mathscr{T}_k = \frac{\tanh k}{2k}. \tag{2.6}$$

The forcing term in (2.4) is assumed to create some mean defect vorticity profile, $F(\eta)$. The linear stability of such a profile is then determined by writing

$\mathscr{Z}(x, \eta, t) = F(\eta) + Z(\eta, t)\,\mathrm{e}^{\mathrm{i}kx}$, and retaining only linear terms in Z; k is the streamwise wavenumber. This leads to the linear vorticity defect equation,

$$Z_t + + \mathrm{i}k\eta Z - \mathrm{i}kF'\mathscr{T}_k \int_{-\infty}^{\infty} Z(\eta', t)\,\mathrm{d}\eta' = \nu Z_{\eta\eta}. \tag{2.7}$$

Equation (2.7) is the central equation of this study. It is similar to a model of Lenard & Bernstein (1958) for waves in a diffusive plasma.

3. Inviscid normal modes

Before approaching the viscous theory and its inviscid limit, it is first helpful to review the stability properties of inviscid defects. The inviscid linear dynamics is governed by the Vlasov-like equation,

$$Z_t + \mathrm{i}k\eta Z = \mathrm{i}kF'\mathscr{T}_k \int_{-\infty}^{\infty} Z(\eta')\,\mathrm{d}\eta', \tag{3.1}$$

which was discussed in depth in paper I. The inviscid normal modes, $Z(\eta, t) = z(\eta)\,\mathrm{e}^{-\mathrm{i}kct}$, where $c = c_r + \mathrm{i}c_i$, satisfy

$$(\eta - c)z = F'\mathscr{T}_k \int_{-\infty}^{\infty} z(\eta')\,\mathrm{d}\eta' \tag{3.2}$$

Provided $c_i \neq 0$, or $\eta - c$ vanishes where $F' = 0$, the eigenfunction may be written in the form

$$z = \mathscr{T}_k \frac{F'(\eta)}{\eta - c} \int_{-\infty}^{\infty} z(\eta')\,\mathrm{d}\eta'. \tag{3.3}$$

Thus, the inviscid dispersion relation is

$$\mathscr{D}_I(c) = 1 - \mathscr{T}_k \int_{-\infty}^{\infty} \frac{F'(\eta)}{\eta - c}\,\mathrm{d}\eta = 0. \tag{3.4}$$

A crucial feature of this dispersion relation is that it is non-analytic in c. In fact, the integrand in (3.4) is singular if c is real. Consequently, the function $\mathscr{D}_I(c)$ is analytic in the upper and lower half-planes, but it has a branch cut along the real axis. The branch cut locates the continuous spectrum of the inviscid problem (Case 1960).

A convenient example is furnished by the Lorentzian profile, $F = f/[\pi(1 + \eta^2)]$. In this particular case, the dispersion relation can be reduced to

$$\mathscr{D}_I(c) = \begin{cases} \mathscr{D}_+(c) = 1 - \rho(c + \mathrm{i})^{-2} & \text{if} \quad c_i > 0 & (3.5a) \\ \mathscr{D}_-(c) = 1 - \rho(c - \mathrm{i})^{-2} & \text{if} \quad c_i < 0, & (3.5b) \end{cases}$$

where $\rho = f\mathscr{T}_k$. The appearance of the sign of c_i in the dispersion relation reflects the non-analytic nature of $\mathscr{D}(c)$, and the branch cut along $c_i = 0$. On solving (3.5), one finds

$$c = \begin{cases} -\mathrm{i} \pm \rho^{1/2} & \text{if} \quad c_i > 0 & (3.6a) \\ \mathrm{i} \pm \rho^{1/2} & \text{if} \quad c_i < 0. & (3.6b) \end{cases}$$

These solutions for c are compatible with the condition on c_i provided $\rho < -1$, in which case, $c = \pm\mathrm{i}(|\rho|^{1/2} - 1)$. That is, a pair of modes: one growing, one decaying. If $\rho > -1$, there are no discrete eigenvalues.

The functions $\mathscr{D}_\pm$ are the analytic pieces of $\mathscr{D}_I$ in the upper and lower halves of the complex plane. The piece, $\mathscr{D}_+$, has solutions (3.6a) over the whole of the complex

plane, but only where $c_i > 0$ are they roots of the true dispersion relation. In the lower half-plane, $\mathscr{D}_+$ is the analytic continuation of $\mathscr{D}$ through the branch cut on the real axis; its zeros with $c_i < 0$ are therefore roots of the imviscid dispersion relation on another Riemann sheet.

Although not true eigenmodes, the objects corresponding to the zeros of $\mathscr{D}_+(c)$ in the lower half-plane appear in the solution of the initial value problem (paper I). In plasma physics, these objects are termed 'quasi-modes', since their form is not separable in η and t; the associated vorticity fluctuation partly has the form $z \propto \exp(-ik\eta t)$. Thus, the vorticity becomes ever more finely crenelated as time proceeds. These modes are also important in the inviscid limit of the viscous problem.

4. Viscous normal modes

4.1. *The dispersion relation*

The viscous normal modes, $Z(\eta, t) = z(\eta)\,\mathrm{e}^{-ikct}$, satisfy

$$v z_{\eta\eta} - ik(\eta - c)z = -ik\mathscr{T}_k\, F'(\eta) \int_{-\infty}^{\infty} z(\eta')\,\mathrm{d}\eta'. \tag{4.1}$$

On introduction of the Fourier transform in η of $z(\eta)$,

$$\hat{z}(q) = \frac{1}{2\pi} \int_{-\infty}^{\infty} z(\eta)\,\mathrm{e}^{-iq\eta}\,\mathrm{d}\eta, \tag{4.2}$$

equation (4.1) is transformed into the first-order equation

$$\frac{\mathrm{d}\hat{z}}{\mathrm{d}q} - \left(\frac{v}{k}q^2 - ic\right)\hat{z} = 2\pi\mathscr{T}_k\, q\hat{F}(q)\hat{z}(0), \tag{4.3}$$

where $\hat{F}(q)$ is the Fourier transform of $F(\eta)$. Equation (4.3) is readily solved:

$$\hat{z}(q) = -2\pi\mathscr{T}_k\,\hat{z}(0)\,\mathrm{e}^{vq^3/3k - icq} \int_{q}^{\infty} \mathrm{e}^{-v\tilde{q}^3/3k + ic\tilde{q}}\hat{F}(\tilde{q})\tilde{q}\,\mathrm{d}\tilde{q}, \tag{4.4}$$

for $k > 0$. Moreover, by taking $q = 0$ and avoiding a trivial solution, one obtains the dispersion relation

$$\mathscr{D}_k(c) = 1 + 2\pi\mathscr{T}_k \int_{0}^{\infty} \mathrm{e}^{-v\tilde{q}^3/3k + ic\tilde{q}}\hat{F}(\tilde{q})\tilde{q}\,\mathrm{d}\tilde{q} = 0. \tag{4.5}$$

This dispersion relation is a powerful result that is exploited in the sections to come.

Once (4.5) is solved for the eigenvalue, c, the eigenfunction results on transforming (4.4) back into physical space:

$$z(\eta) = -2\pi\mathscr{T}_k \int_{-\infty}^{\infty} \mathrm{d}q\,\mathrm{e}^{iq\eta + vq^3/3k - icq} \int_{q}^{\infty} \mathrm{e}^{-v\tilde{q}^3/3k + ic\tilde{q}}\hat{F}(\tilde{q})\tilde{q}\,\mathrm{d}\tilde{q}, \tag{4.6}$$

if the eigenfunction is scaled such that $\hat{z}(0) = 1$.

4.2. *The Couette problem*

If $F(\eta) \equiv 0$, then equation (4.6) becomes trivial, indicating that the defect Couette problem has no normal mode solutions. In this case, the meaning of the defect is as a localized perturbation to the Couette background. The reason why there are no normal modes is seen on considering the general solution to (2.7) with $F(\eta) = 0$:

$$Z(\eta, t) = \mathrm{e}^{-ik\eta t} \int_{-\infty}^{\infty} \hat{Z}_0(q)\,\mathrm{e}^{v[(q-kt)^3 - q^3]/3k + iq\eta}\,\mathrm{d}q \tag{4.7}$$

(Kelvin 1887; Orr 1907), where $\hat{Z}_0$ is the transform of the initial condition. Equation (4.7) can be interpreted as an integral superposition of the eigenmodes of a continuous spectrum, eigenmodes whose structure is not separable in η and t. Thus the defect Couette problem has a continuous spectrum rather than discrete normal modes.

The continuous spectrum of the Couette defect is surprising in view of the fact that the Orr–Sommerfeld problem in a finite channel has discrete eigenvalues (Murdock & Stewartson 1978). This arises because the matched asymptotic expansion used here recasts the problem on an infinite domain, but this is not physically serious. The Orr–Sommerfeld modes that are not captured by the defect theory are either unlocalized and decay much more rapidly than the modes that are left in (Schmid *et al.* 1993), or are concentrated in boundary layers near the walls (Davey 1973) where they describe local viscous relaxation to the condition of the boundary, not properties of the shear dynamics. In other words, the asymptotic theory filters the rapidly decaying modes and decouples the defect physics from the walls.

5. Stability characteristics of viscous defects

5.1. *Sample profiles*

Three sample defect profiles are shown in figure 2. These are a member of the family of Lorentzian-like profiles,

$$F(\eta) = f \frac{(1 + \alpha\eta + \beta\eta^2)}{\pi(1 + \eta^2)^2}, \tag{5.1}$$

a Gaussian,

$$F(\eta) = \left(\frac{2}{\pi}\right)^{1/2} f e^{-\eta^2/2}, \tag{5.2}$$

and a defect given by

$$\hat{F}(q) = \frac{1}{2\pi} |q| f e^{-|q|^3/3}. \tag{5.3}$$

In these formulae, f, α and β are various parameters. When $\alpha = 0$ and $\beta = 1$, the profile (5.1) reduces to the Lorentzian. For the final example, the spatial dependence of the profile is given only as an integral, but it yields stability boundaries that can be written in closed form.

For these profiles, the dispersion relation can be written as a relatively simple integral. For example, with profile (5.1), the associated dispersion relation takes the form

$$\mathcal{D}_k(c) = 1 + \tfrac{1}{2}\rho \int_0^\infty e^{-\mu q^3 - icq - q} [1 + \beta + q(1 - \beta) - i\alpha q] q \, dq = 0. \tag{5.4}$$

In addition to the 'shape parameters' α and β, this dispersion relation contains the two parameters $\rho = f\mathcal{T}_k$ and $\mu = \nu/3k$. The corresponding dispersion relations for (5.2) and (5.3) also contain two parameters like ρ and μ. In principle, one could therefore write down a reduced set of parameters upon which the stability properties depend; however, this will not be done here. The dispersion relations can be solved numerically by evaluating the integral with a suitable quadrature rule.

5.2. *The zoo of instabilities*

Given the dispersion function, $\mathcal{D}_k(c)$, it is possible to formulate a Nyquist method to determine the stability of a given profile (cf. Penrose 1960; paper I). This method consists of drawing the function $\mathcal{D}_k(c) = \mathcal{D}_r(c) + i\mathcal{D}_i(c)$ on the $(\mathcal{D}_r, \mathcal{D}_i)$-plane for c
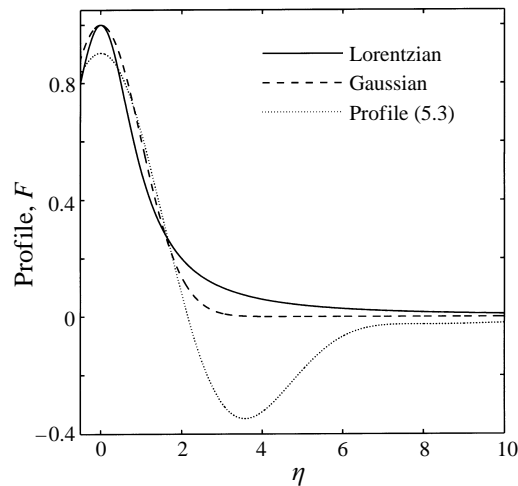
FIGURE 2. Sample profiles used in the stability analysis (profile (5.1) with $\alpha = 0$, $\beta = 1$).

varying along the real axis. As $c \rightarrow \pm\infty$, $\mathscr{D}_k \rightarrow 1$, and so the resulting curve, or *locus*, begins and ends at the point $(1,0)$ on this plane. If, in the interim excursion across the $(\mathscr{D}_r, \mathscr{D}_i)$-plane, the locus encircles the origin, then there is an exponentially growing mode. If the locus circles around the origin more than once, then there are correspondingly many unstable modes.

Some Nyquist plots for the Lorentzian family are shown in figure 3. In these cases, the loci encircle the origin, hence the profiles are unstable. In fact, the second Nyquist plot encircles the origin *twice*, signifying two instabilities. Note that the first example has a single minimum in vorticity, that is, an *inflection point* of the velocity profile. Also, the associated Nyquist plot has a single principal loop. For the second example, there are two principle minima and there are two main loops to the Nyquist plot. These instabilities are therefore associated with the primary minima of the vorticity distribution; they are what one might call 'primary instabilities'.

For the profiles of figure 3, increasing the effective dissipation, $\mu = \nu/3k$, causes the locus to shrink. Hence viscosity plays a stabilizing role, but this is not always the case. Figure 4 shows plots for a profile with $\alpha = 0$ and $\beta = 1.95$. For this value of β, the Nyquist plot at small μ contains a 'kink' near the origin. If the dissipation, μ, is increased, this kink straightens out, with the result that the curve encloses the origin at larger μ. In other words, viscosity *destabilizes* this profile, at least at small enough μ.

The reason why viscosity plays a stabilizing role in this example is connected to interactions amongst the eigenmodes. The unstable mode indicated in figure 4 is on the brink of coalescing with a second, damped, real mode to produce a complex conjugate pair; reducing the viscosity has the effect of accelerating the coalescence (which 'drags' the eigenvalues together) rather than decreasing the damping of the mode. The complex conjugate pair itself can become unstable for different parameter values. In fact, the profile is close to a 'degenerate' profile with $F'(0) = F''(0) = F'''(0) = 0$, which can be modified such that two new inflection points appear. For the degenerate profile, the coalescing modes can bifurcate to instability exactly at the point for which they coalesce (that is, a 'Takens–Bogdanov' bifurcation). In the Nyquist plots, this higher-order bifurcation is revealed by the creation of a second loop at the 'kink'.
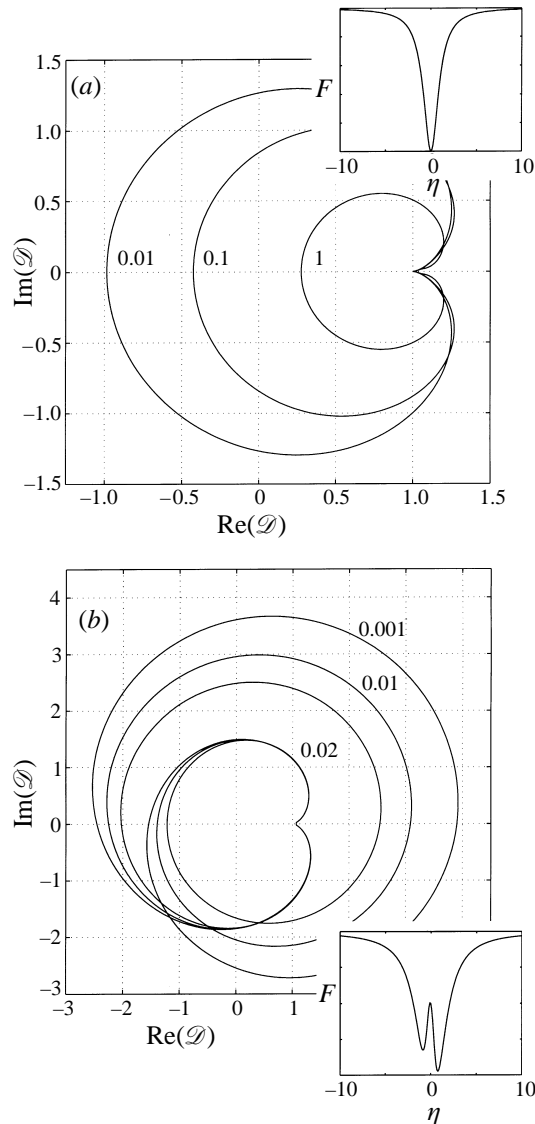
FIGURE 3. Nyquist plots for the Lorentzian family (5.1) with $\rho = f \tanh k/2k = -2$. (a) $\alpha = 0$ and $\beta = 1$, and $v/k = 0.001$, 0.1 and 1. (b) $\alpha = 0.5$ and $\beta = 5$, and $v/k = 0.02$, 0.01 and 0.001. The insets show the profile, $F(\eta)$.

This is one example of how more complicated (higher codimension) bifurcations can be uncovered by Nyquist theory.

The Nyquist plots also uncover a variety of different types of instabilities. Other examples are shown in figures 5 and 6. In figure 5, the instability arises as a result of a secondary minimum in the vorticity distribution. This instability persists in the inviscid limit (see §5.3), where it is analogous to the 'bump-on-tail' instability of plasma physics (see paper I). In figure 6, there is a pair of unstable modes associated with loops of the Nyquist plot that exist only for larger v/k, and when the profile has a *maximum*. The instability is not directly associated with any vorticity minima, and is quite different from the other types of instabilities signified by figures 3–5. For
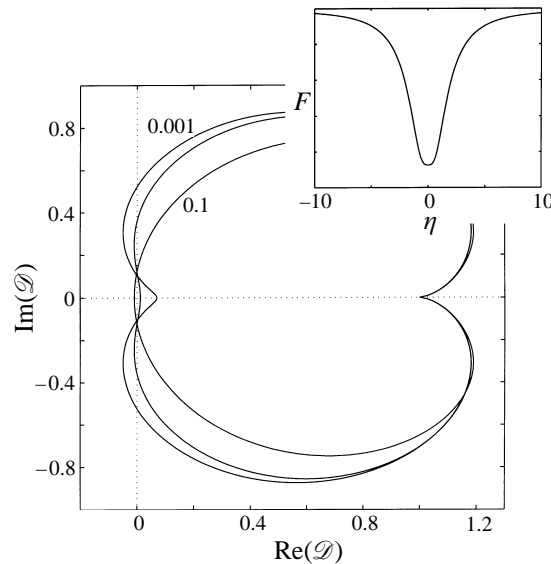
FIGURE 4. Nyquist plot for profiles (5.1) with $\alpha = 0$, $\beta = 1.95$ and $\rho = -1.75$.
The three curves correspond to $\mu = 0.001$, 0.01 and 0.1.

symmetrical profiles like (5.1)–(5.3), the two modes are complex conjugates; that is, waves travelling in opposite directions (the double loop of the Nyquist plot reflects a Hopf bifurcation).

5.3. *Stability boundaries*

Stability boundaries for the primary instabilities of profiles from the three families (5.1)–(5.3) are illustrated in figure 7. These are shown on the $(k, 1/v)$-plane for given f ($1/v$ is the 'defect Reynolds number'). For profile (5.3), the stability boundary is given in closed form by the relation

$$\rho = f\mathscr{T}_k = -(1 + v/k). \tag{5.5}$$

As $v \to 0$, the primary mode expands to cover a finite band of wavenumbers. Also shown on the figure is the stability boundary of the inviscid theory. As is well known, the inviscid theory captures the upper stability boundary, but not that at $k = 0$. This is connected to the absence of an inviscid limit at $k = 0$ (§ 6). The primary instabilities are therefore viscous extensions of Rayleigh's classical inflection-point instabilities.

In figure 8, the stability boundary of the 'bump-on-tail' mode is drawn. In contrast to the case for the primary instabilities, the inviscid theory predicts both stability boundaries. Also, the unstable band actually widens to smaller values of k on *increasing* v at the highest Reynolds numbers. That is, viscosity again plays a destabilizing role. This is also true for the example of figure 9, which displays the stability boundaries for modes related to the unstable pair of figure 6. For this final case, as $v \to 0$, the unstable range shrinks to an infinitely narrow band with $k \to 0$. The instability is not present in the inviscid theory and is an example of a viscously catalysed instability: that is, viscous overstability.

In summary, simple profiles like the Lorentzian or Gaussian have primary modes of instability associated with vorticity minima, and secondary, viscously catalysed modes. In fact, this terminology carries over to much more general classes of profiles. For profiles with more inflection points there are more principal loops to the Nyquist
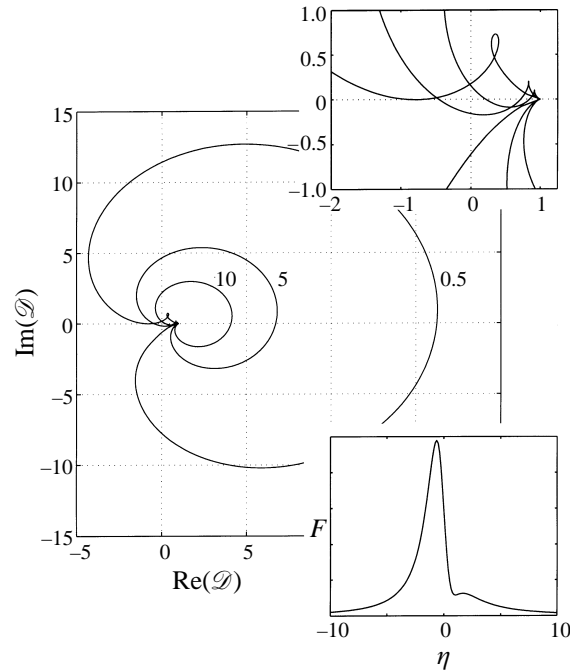
FIGURE 5. Nyquist plot for the profile (5.1) with $\alpha = -2.2$, $\beta = 2$, $f = 10$ and $v = 0.1$. The three plots are shown correspond to $k = 0.5$, 5 and 10. The insets shows a magnification of the plot near the origin and the profile itself.

plot (e.g. figure 1), leading to the possibility of further primary modes of instability. Furthermore, these primary modes are expected to limit to inviscid instabilities as $v \to 0$ (§6). In addition, when the profile is more complicated, there may be more secondary loops in the Nyquist plot, signifying a multiplication of viscously catalysed instabilities. But as $v \to 0$, the bands of these instabilities shrink to $k = 0$.

5.4. *Eigenspectra*

The Nyquist plots give an indication of the instabilities to which a particular profile is prone. However, the full eigenspectrum also contains many other modes. The eigenspectra for profiles of the three families (5.1)–(5.3) are illustrated in figure 10: shown are the eigenvalues closest to the real axis. Some of the eigenfunctions for the Lorentzian profile (equation (5.1) with $\alpha = 0$ and $\beta = 1$) are displayed in figure 11.

The spectrum of each profile consists of a sequence of eigenvalues lying near a 'wedge' on the spectral plane. These modes can be approximately constructed by using the method of stationary phase to reduce the dispersion relation (Appendix A). For the Lorentzian profile, this gives the approximate relation,

$$c \sim -\mathrm{i} + \left(\frac{9v\pi^2 n^2}{4k} \right)^{1/3} \mathrm{e}^{-\mathrm{i}\pi/2 \pm \mathrm{i}\pi/3}, \tag{5.6}$$

for n an odd integer if $\rho > 0$, and even if $\rho < 0$ (see Appendix A). Thus the modes of profiles with $\rho > 0$ and $\rho < 0$ asymptotically lie interwoven along a common curve (cf. figure 10a), and are separated by an amount $v^{1/3}n^{-1/3}$. This suggests that there
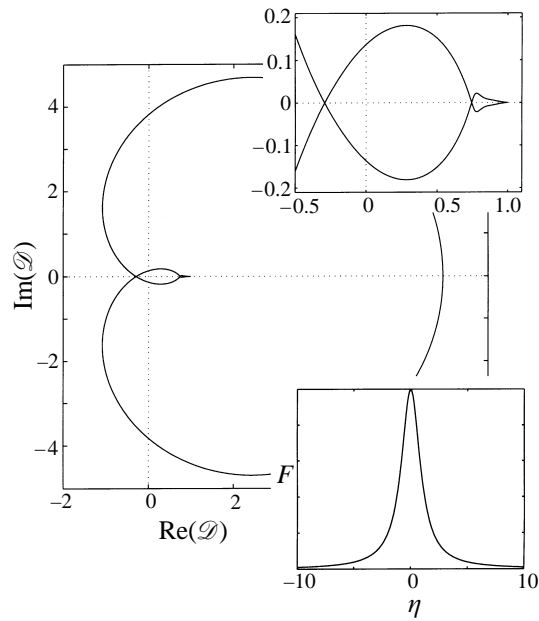
FIGURE 6. Nyquist plot for the Lorentzian profile with $\rho = 100$ and $\nu/k = 40$. The insets shows a magnification of the plot near the origin and the profile itself.
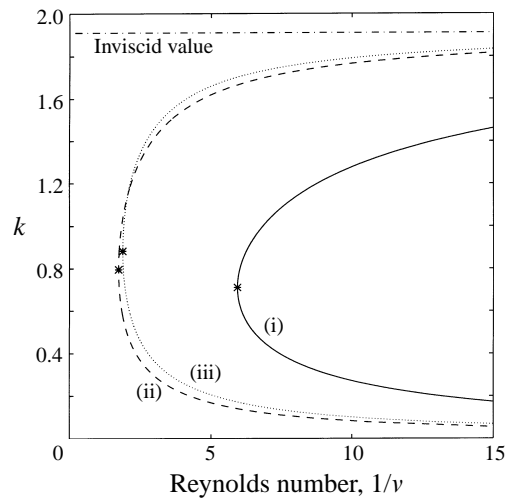

FIGURE 7. Stability boundaries for the primary mode of three profiles of families (5.1)–(5.3) ($\alpha = 0$, $\beta = 1$), with $f = -2$. The inviscid stability boundary is also indicated (it is the same for all three profiles).

is an infinite number of modes distributed near the wedge. Moreover, as $\nu \to 0$, the separation decreases to zero, implying that the modes condense into a continuous spectrum on the edge of the wedge itself.

For the Gaussian profile, the modes follow an asymptotic relation,

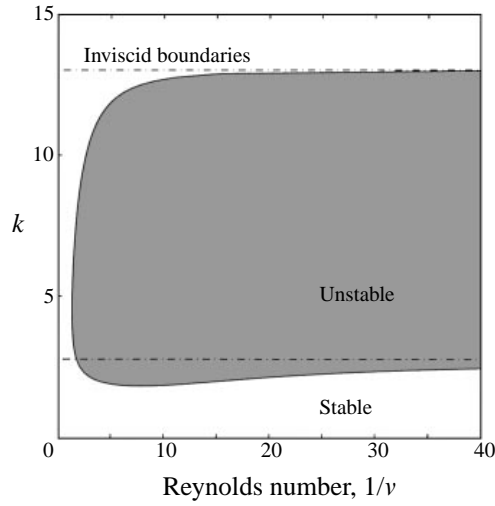$$c \sim -(\mathrm{i} \pm 1)[(n + 1/4)\pi]^{1/2}, \tag{5.7}$$

FIGURE 8. Stability boundaries for the 'bump-on-tail' mode implied by figure 6 ($\alpha = -2.2$, $\beta = 2$, $f = 50$). The inviscid stability boundaries are also indicated.
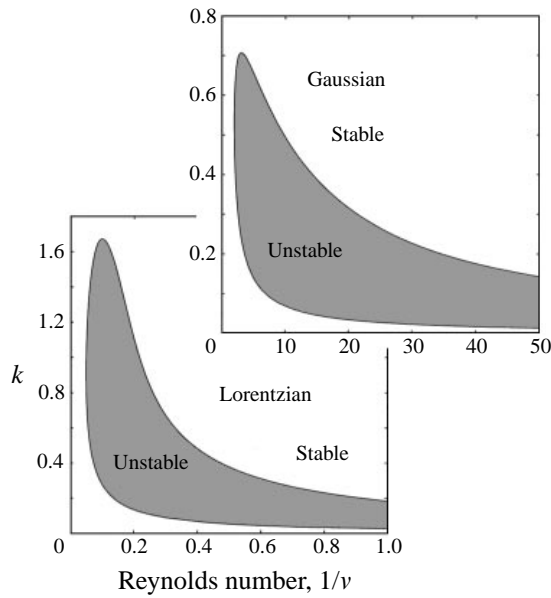
FIGURE 9. Stability boundaries for viscously catalysed double instabilities. The two pictures show the boundaries for the Lorentzian profile with $f = 150$ ($\alpha = 0$, $\beta = 1$), and Gaussian with $f = 20$.

and for the profile (5.3),

$$c \sim \left[\frac{9\pi^2 n^2}{4}(1 + v/k)\right]^{1/3} e^{-i\pi/2 \pm i\pi/3} \tag{5.8}$$

(Appendix A). In the limit $v \to 0$, these modes remain equally spaced, so there is no creation of a continuum.

These examples show that the eigenmodes of the viscous defect have no special universal distribution, other than that they seem typically to line up beside some

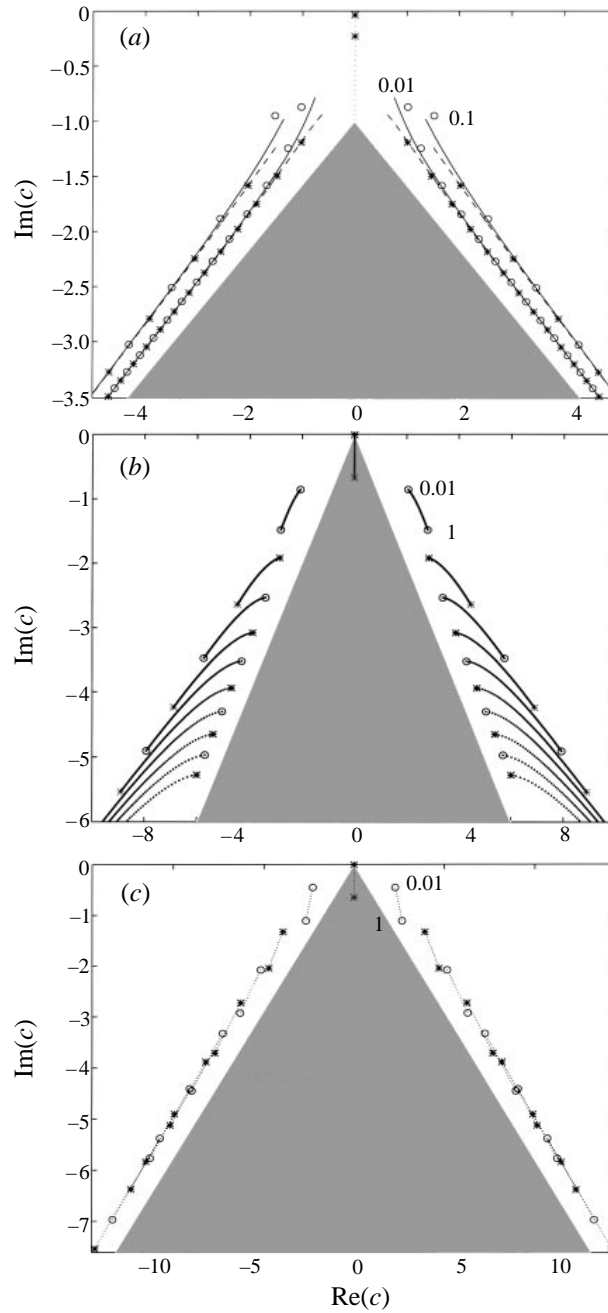FIGURE 10. Eigenvalue spectra. (*a*) The spectrum of the Lorentzian profile. Two sets of eigenvalues are shown: one set corresponds to $v/k = 0.1$, the other to $v/k = 0.1$. The circles show the eigenvalues for $\rho = 1$ and the stars those for $\rho = -1$. The asymptotic 'curves' given by (A 8) and (A 9) for $\rho = \pm 1$ are drawn solid and dashed. (*b*) Spectra for the Gaussian profile: eigenvalues for v/k varying between 0.01 and 1, and for $\rho = \pm 1$. The stars show the spectrum at $v/k = 0.01$ and 1 for $\rho = -1$, and the circles that for the same values of v/k but with $\rho = 1$. (*c*) Spectra for the profile (5.3) in the same manner as in (*b*). Only the lowest-order eigenvalues are displayed in each case, and on each picture, a shaded area indicates a 'wedge' besides which the eigenvalues line up.
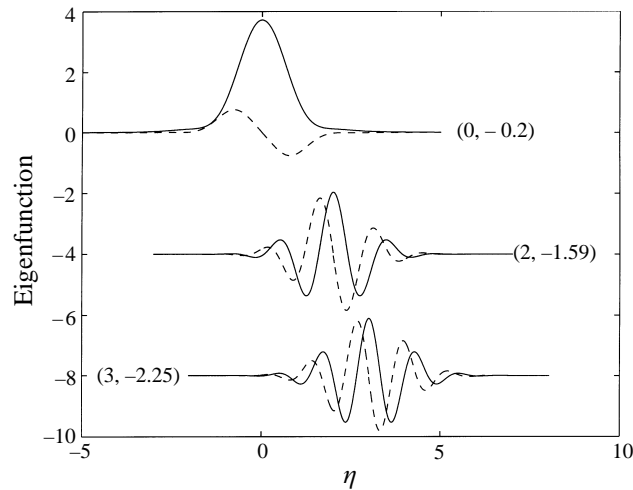
FIGURE 11. Eigenfunctions of the Lorentzian profile for $\mu = 0.1$. Three eigenfunctions labelled by their eigenvalues are shown; two are offset and all are suitably scaled to allow a comparison. The real parts are drawn as continuous curves, imaginary parts as dashed curves.

wedge on the spectral plane, and that there are distinguished modes near the apex of the wedge that are responsible for instability. The important factor controlling the form of the spectrum is the exponent of the decay of the Fourier transform of the vorticity distribution. In any event, the limiting viscous eigenspectrum does not appear to have any correspondence with the spectrum of the inviscid problem. Any connections are made more explicit in the next section.

6. The inviscid limit

The goal of this section is to take the inviscid limit of the defect equation. The main problem with taking this limit is that the viscosity is a singular perturbation to the inviscid problem and there is no reason to expect that the solutions to the two problems to correspond. Indeed, by setting $v = 0$ in the dispersion relation (4.5), one removes the dominant exponential term that can be responsible for the convergence of the integral.

A further problem in taking the inviscid limit is that the controlling parameter of viscous theory is not actually v, but is really v/k. Hence various inviscid limits are possible, depending on the ratio v/k. Here, the limit $v/k \to 0$, or $v \to 0$ at fixed k, is taken to be the inviscid limit. This indicates that the zero-wavenumber modes are never contained in the theory described in this section. In fact, for $v \to 0$ and $k \to 0$ with $\mu = v/3k$ finite, the problem does not change at all, which is why the inviscid theory fails to account for the lower stability boundaries of the primary modes of instability in figure 7.

6.1. *The limiting Lorentzian spectrum*

For the Lorentzian profile the inviscid theory has an explicit dispersion relation (§ 3), and it is useful to consider this case in detail. In the viscous theory, the Lorentzian profile has the dispersion relation in (5.4) (with $\alpha = 0$ and $\beta = 1$). On taking $v/k \to 0$,

and inserting the large-argument expansion (A 2) of the integral, one obtains

$$1 = \frac{\rho}{(c+\mathrm{i})^2} \sum_{n=0}^{\infty} \frac{(3n+1)!(\mathrm{i}v/k)^n}{3^n n!(\mathrm{i}+c)^{3n}} \quad \text{if} \quad c \in S. \tag{6.1}$$

The allowed sector, S, in (6.1) is the region in the c-plane outside the 'wedge' beside which the eigenvalues tend to line up in figure 10(*a*); that is, the region $-5\pi/6 < \mathrm{Arg}\,(c+\mathrm{i}) < -\pi/6$. The restriction that $c \in S$ in (6.1) arises because of the two expansions for the integral in (A 2) and (A 3).

To leading order in v/k, the approximation (6.1) is

$$\mathscr{D}_v(c) = 1 - \rho(c+\mathrm{i})^{-2} \quad \text{if} \quad c \in S. \tag{6.2}$$

The inviscid dispersion relation can be written in the form

$$\mathscr{D}_I(c) = \mathscr{D}_\pm(c) = 1 - \rho(c \pm \mathrm{i})^{-2}, \quad c_i \gtrless 0. \tag{6.3}$$

Whereas the inviscid relation in (6.3) is a non-analytic function of c with a branch cut along the real axis ($c_i = 0$), the slightly viscous dispersion relation in (6.2) is analytic in c (though there is an exponentially large term that has been left out if c lies inside the wedge rather than S). In fact, $\mathscr{D}_v \equiv \mathscr{D}_+$, but whereas $\mathscr{D}_+$ is valid in only the upper half-plane for the inviscid problem, $\mathscr{D}_v$ is valid everywhere but inside the wedge.

If $\rho < -1$, the inviscid relation has a pair of conjugate eigenvalues. The unstable eigenvalue solves $\mathscr{D}_+(c) = 0$, and so it is also the limit of a viscous mode. However, the damped inviscid mode solves $\mathscr{D}_-(c) = 0$, and has no viscous counterpart. This just reiterates the commonly accepted belief that the decaying mode is a manifestation of the time-reversibility of the inviscid system, and is not causally acceptable on the addition of viscosity, but the instability is permitted (Lin 1945, 1955).

If $\rho > -1$, then the inviscid relation has no eigenvalues. However, $\mathscr{D}_+(c) = 0$ has two solutions that are the inviscid quasi-modes. Somewhat curiously, provided they do not lie inside the wedge, these quasi-modes are also solutions of the slightly viscous dispersion relation. Hence, it appears that the addition of a slight viscosity makes the quasi-modes in S into true eigenmodes. This transformation is also revealed in the limiting form of the eigenfunction.

6.2. *Limiting eigenfunctions*

Just as for the dispersion relation, the integrals appearing in the form of the eigenfunction (4.6) can be evaluated asymptotically. This reveals that, for profiles like (5.1)–(5.3),

$$z(\eta) \sim \mathrm{i}\mathscr{T}_k F'(\eta) \int_0^{\infty} \mathrm{e}^{-\mu q^3 - \mathrm{i}(\eta-c)q} \,\mathrm{d}q, \tag{6.4}$$

which shows agreement with numerical calculation (some examples of which are shown in figure 12). When $c_i > 0$, (6.4) reduces further to

$$z(\eta) \sim \frac{\rho F'}{\eta - c}, \tag{6.5}$$

on using the expansion (A 2) of the integral. This is the inviscid eigenfunction, suitably scaled. If $c_i < 0$, then (A 2) cannot be used everywhere. Instead, (A 2) and (A 3) imply

$$z(\eta) \sim \begin{cases} \rho F'/(\eta - c) & \text{if} \quad \eta < -\sqrt{3}c_i \text{ or } \sqrt{3}c_i < \eta \\ \exp[-(4\mathrm{i}k(\eta-c)^3/9v)^{1/2}] & \text{if} \quad -\sqrt{3}c_i < \eta < \sqrt{3}c_i, \end{cases} \tag{6.6}$$

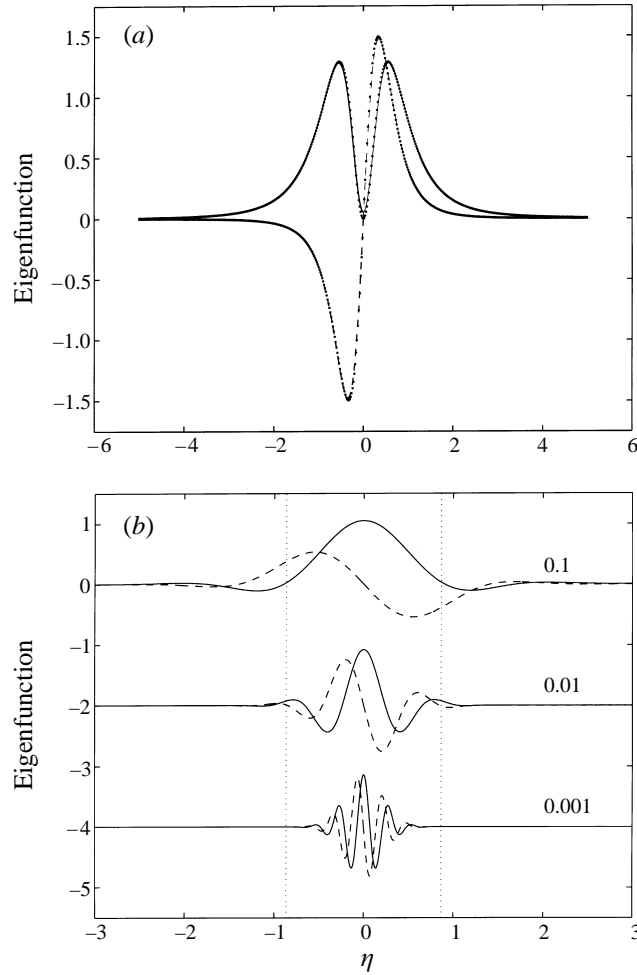which reproduces the trend shown in figure 12.

FIGURE 12. Limiting eigenfunctions for the Lorentzian profile. (*a*) An unstable eigenfunction with $c = (0, 0.5)$, for $\mu = 0.01$ (solid curve for the real part, dashed curve for the imaginary) that limits to the inviscid mode (dots). (*b*) Damped eigenmodes with $c = (0, -0.5)$, for $\mu = 0.1$, 0.01 and 0.001 (solid curves for real parts, dashed for imaginary). The vertical lines indicate $\pm c_i \sqrt{3}$.

As $v \to 0$, the eigenfunctions with $c_i < 0$ therefore oscillate spatially with infinitely short wavelength within some interval of the inviscid critical layer (cf. Stewartson 1981), which suggests an intriguing connection with the quasi-mode form, $\exp(-ik\eta t)$. Outside this interval, though, the rapid oscillations disappear, perhaps reflecting a viscous smoothing of the shearing process described by the quasi-mode. However, these are only qualitative statements aimed at provoking further study.

6.3. *Inviscid limits for general profiles*

In the case of a general profile, if $c_i \geqslant 0$, then one can again asymptotically reduce the dispersion relation. First one transforms $\hat{F}$ in the dispersion relation back into real space:

$$1 = i \mathscr{T}_k \int_{-\infty}^{\infty} F'(\eta) \, d\eta \int_0^{\infty} e^{-vq^3/3k - i(\eta - c)q} \, dq. \qquad (6.7)$$

Since $z = \eta - c$ always lies in the lower half-plane when $c_i \geqslant 0$, the expansion (A 2) of the integral reveals

$$1 = \mathscr{T}_k \sum_{n=0}^{\infty} \frac{(3n)! (\mathrm{i}v/k)^n}{3^n n!} \int_{-\infty}^{\infty} \frac{F_\eta(\eta)\,\mathrm{d}\eta}{(\eta - c)^{3n+1}}, \quad c_i \geqslant 0. \tag{6.8}$$

If $c_i < 0$, then the expansion leading to (6.8) is not valid, and there are certain portions of the path of integration over which one integrates an exponentially large term of the form (A 3).

Equation (6.8) is superficially a non-analytic dispersion relation since each term contains a singular integral with a branch cut along the real axis. Actually, if the fact that (6.8) is not suitable for eigenvalues with $c_i < 0$ is simply ignored, then that formula limits exactly to the inviscid dispersion relation. In other words, one recovers the non-analytic inviscid problem only after an inconsistent treatment of the limits of the analytic viscous problem.

In any event, provided $c_i \geqslant 0$, equation (6.8) furnishes the correct inviscid limits of the viscous eigenvalues, which are, as expected, the inviscid eigenvalues. To find the next-order corrections, one truncates the sum on the right-hand side of (6.8) after the first two terms, then inserts the series $c \sim c_0 + vc_1$, where c_0 is the inviscid eigenvalue. This gives

$$kc_1 \int_{-\infty}^{\infty} \frac{F_\eta(\eta)\,\mathrm{d}\eta}{(\eta - c_0)^2} = -2\mathrm{i} \int_{-\infty}^{\infty} \frac{F_\eta(\eta)\,\mathrm{d}\eta}{(\eta - c_0)^4} \tag{6.9}$$

for an unstable mode, and

$$kc_1 \left[\mathscr{P} \int_{-\infty}^{\infty} \frac{F_\eta(\eta)\,\mathrm{d}\eta}{(\eta - c_0)^2} + \mathrm{i}\pi s F^{ii} \right] = -2\mathrm{i} \left[\mathscr{P} \int_{-\infty}^{\infty} \frac{F_\eta(\eta)\,\mathrm{d}\eta}{(\eta - c_0)^4} + \mathrm{i}\frac{\pi}{6} s F^{iv} \right], \tag{6.10}$$

for a neutral one, where $\mathscr{P}$ signifies the Cauchy principal value, s is the sign of $\mathrm{Im}\,(c_1)$ and

$$F^{ii} = \left[\frac{\mathrm{d}^2 F}{\mathrm{d}\eta^2} \right]_{\eta = c_0} \quad \text{and} \quad F^{iv} = \left[\frac{\mathrm{d}^4 F}{\mathrm{d}\eta^4} \right]_{\eta = c_0}. \tag{6.11}$$

To concentrate on the inviscid neutral modes, equation (6.10) implies the eigenvalue correction

$$k_0 c_1 = 2\mathrm{i} \frac{Q_3 + \mathrm{i}\pi s F^{iv}/6}{Q_1 + \mathrm{i}\pi s F^{ii}}, \tag{6.12}$$

where

$$Q_n = \mathscr{P} \int_{-\infty}^{\infty} \frac{F_\eta(\eta)\,\mathrm{d}\eta}{(\eta - c_0)^{n+1}}. \tag{6.13}$$

Equation (6.12) gives the viscous perturbation of the inviscid neutral mode. It provides the eigenvalue correction as a function of the underlying equilibrium state. Importantly, the effect of viscosity is not definite in sign, indicating that the addition of dissipation may either damp or destabilize the neutral mode. For example, for symmetrical profiles and $c_0 = 0$, the integrals Q_1 and Q_3 vanish, leaving

$$k_0 c_1 = \frac{\mathrm{i} F^{iv}}{3 F^{ii}}. \tag{6.14}$$

In the specific case of the Lorentzian, $k_0 c_1 = -f$, and so viscosity damps the inviscid neutral mode. For general, symmetrical profiles, (6.14) implies that the effect of viscosity depends on the sign of F^{ii}/F^{iv}. That is, this aspect of the shape of the profile

at the inflection point determines whether viscosity damps or destabilizes the mode, a rather pleasant (if a little curious) result. (The profile of figure 4 has $F^{iv}/F^{ii} > 0$.)

6.4. *Limits to quasi-modes*

In general, the perturbation scheme outlined above is useful only if the perturbed modes have $c_i \gtrsim 0$, and so it establishes the connection between inviscid instabilities and limiting viscous ones. If $c_i < 0$, the sum (6.8) is not valid. This is unfortunate since one cannot then make a definite connection between the limit of a viscous mode and the quasi-modes of inviscid theory. The important feature of the Lorentzian that leads to this connection is the Fourier transform of the profile, $e^{-|q|}$. The decay of $\hat{F}(q)$ extends the region of the c-plane over which the integral in the dispersion relation converges to its value for $v/k = 0$. It then follows that the asymptotic approximation (6.1) is valid if c lies outside the wedge. That is, the limiting viscous dispersion relation has the form of the analytically extended inviscid relation, $\mathscr{D}_+(c)$, in S.

A stronger result follows for the Gaussian and profile (5.3). In these cases, the integral in the dispersion relation converges to its value at $v/k = 0$ over the entire c-plane. The asymptotic form of the integral therefore becomes independent of v, resulting in a limiting dispersion relation,

$$\mathscr{D}_v(c) \sim 1 + 2\pi\mathscr{T}_k \int_0^\infty e^{ic\tilde{q}}\hat{F}(\tilde{q})\tilde{q}\,d\tilde{q} = 0, \qquad (6.15)$$

which is identical to the inviscid dispersion relation, $\mathscr{D}_+$, calculated assuming that $c_i > 0$. In other words, once again $\mathscr{D}_v = \mathscr{D}_+$, though there is now no restriction on the eigenvalue. This indicates that the quasi-modes are once again the limits of viscous modes. In fact, the modes shown in figures 10(*b*) and 10(*c*) all limit to quasi-modes.

Thus, in general, there are a whole classes of profiles for which the quasi-modes are the limits of viscous modes. Related remarks for the solutions of the Orr–Sommerfeld equation are given by Stewartson (1981). Quasi-modes are not, however, always the limits of viscous modes (the quasi-mode of the Lorentzian that lies inside the wedge when $\rho < 0$ is not, for example, a viscous mode).

7. Beyond normal modes

7.1. *Weakly nonlinear theory*

Finally, two further aspects of the stability theory are briefly considered. The first is weakly nonlinear theory.

Thus far, this study has concentrated on infinitesimal perturbations to the shear flow. With the relatively simple defect equation, however, one can open a weakly nonlinear expansion in a straightforward way. This generates an asymptotic amplitude equation governing the development of the instability. Although the coefficients of this equation are not given in closed form even for the defect theory, they do have the form of simple quadratures. The calculation is a standard one for viscous defects, and for that reason, it is relegated to Appendix B. The salient result is the following: If one sets $v = v_0 + \delta^2 v_2$, with $\delta \ll 1$ and for $k = k_0(v_0, f)$ a point on the stability boundary, then there is a distinguished mode, $\delta A(T)z(\eta)e^{ik_0 x} + \text{c.c.}$, that evolves on a slow time scale, $T = \delta^2 t$. The evolution equation for $A(T)$ is the Landau equation,

$$A_T = \gamma A + \varpi |A|^2 A \qquad (7.1)$$

(cf. Stuart 1960), with γ and ϖ given by the integrals (B 19) and (B 20) of Appendix B.

For *all* of the instabilities uncovered in §5, numerical evaluation of the real part of the nonlinear coefficient, ϖ, reveal it to be negative near the point of marginal stability, although the criticality changes over the stability boundary. Thus, near marginality the instabilities are *supercritical*. Hence, out of the stability boundary one expects a stable branch of finite-amplitude solutions to bifurcate. Whether this kind of behaviour is a general property of viscous defects is not clear. It is in contrast to the situation normally conjectured in shear flow instability (Stuart 1960), but it is in accord with preliminary numerical studies (del Castillo-Negrete, Young & Balmforth 1995). In fact, for the full shear flow problem the sign of the cubic coefficient apparently depends on factors such as the shape of the profile, and previous studies have found both subcritical and supercritical instability (see Drazin & Reid 1981). In other words, the controlling influences on the criticality of the instability are not well understood; the defect theory provides a simple framework to explore the issue.

7.2. *The initial-value problem*

Another important facet of the problem that has only been indirectly touched upon is the study of the linear initial-value problem. Just as the normal mode problem can be reduced to an explicit dispersion relation, the linear defect equation can be also solved with Laplace transform techniques.

The Laplace transform of equation (2.7) is

$$v\frac{\partial^2}{\partial\eta^2}Z_p - pZ_p - ik\eta Z_p = -ikF'(\eta)\mathscr{T}_k\int_{-\infty}^{\infty} Z_p\mathrm{d}\eta' - Z_0(\eta), \qquad (7.2)$$

where p is the transform coordinate, $Z_p(\eta,p)$ is the transform of $Z(\eta,t)$, and $Z_0(\eta) = Z(\eta,t=0)$ is the arbitrary initial condition. Equation (7.2) can be solved on Fourier transforming in η:

$$\frac{\mathrm{d}}{\mathrm{d}q}\hat{Z}_p - \frac{1}{k}(vq^2 + p)\hat{Z}_p = 2\pi\mathscr{T}_k\tilde{F}q\hat{Z}_p(0,p) - \hat{Z}_0(q), \qquad (7.3)$$

where $\hat{Z}_p(q,p)$ is the Fourier transform of $Z_p(\eta,p)$ and $\hat{Z}_0(q)$ that of $Z_0(\eta)$. Equation (7.3) integrates to

$$\hat{Z}_p(q,p) = -\mathrm{e}^{vq^3/3k+pq/k}\int_q^{\infty}\mathrm{e}^{-v\tilde{q}^3/3k-p\tilde{q}/k}\left[\frac{1}{k}\hat{Z}_0(\tilde{q}) - 2\pi\mathscr{T}_k\hat{F}(\tilde{q})\tilde{q}\hat{Z}_p(0,p)\right]\mathrm{d}\tilde{q}. \qquad (7.4)$$

Thus,

$$\hat{Z}_p(0,p) = \frac{\mathscr{N}(p)}{\mathscr{D}(ip/k)}, \qquad (7.5)$$

where

$$\mathscr{N}(p) = \frac{1}{k}\int_0^{\infty}\mathrm{e}^{-vq^3/3k-pq/k}\hat{Z}_0(q)\,\mathrm{d}q \qquad (7.6)$$

and

$$\mathscr{D}(ip/k) = 1 + 2\pi\mathscr{T}_k\int_0^{\infty}\mathrm{e}^{-vq^3/3k-pq/k}\hat{F}(q)q\,\mathrm{d}q \qquad (7.7)$$

is the dispersion relation featured in the earlier parts of this study. The streamfunction at the defect is therefore

$$B(t) = -\mathscr{T}_k\int_{-\infty}^{\infty} Z(\eta,t)\mathrm{d}\eta = -\frac{1}{2\pi i}\mathscr{T}_k\int_{\mathscr{C}}\mathrm{e}^{pt}\frac{\mathscr{N}(p)}{\mathscr{D}(ip/k)}\,\mathrm{d}p, \qquad (7.8)$$

where $\mathscr{C}$ is the Bromwich contour. Similar inverse transforms give the vorticity perturbation at any point in time and space:

$$Z(\eta, t) = e^{-ik\eta t} \int_{-\infty}^{\infty} \hat{Z}_0(q)\, e^{\nu[(q-kt)^3 - q^3]/3k + iq\eta}\, dq + \frac{1}{2\pi i} \int_{\mathscr{C}} e^{pt} \frac{\mathscr{N}(p)}{\mathscr{D}(ip/k)} z(\eta; ip/k)\, dp, \quad (7.9)$$

with

$$z(\eta; c) = -2\pi \mathscr{T}_k \int_{-\infty}^{\infty} e^{\nu q^3/3k - iq(\eta-c)}\, dq \int_{q}^{\infty} e^{-\nu \tilde{q}^3/3k + ic\tilde{q}} \hat{F}(\tilde{q}) \tilde{q}\, d\tilde{q}, \quad (7.10)$$

which is the normal mode eigenfunction if c is an eigenvalue.

When $F \equiv 0$, (7.8) simplifies to

$$B(t) = -\mathscr{T}_k \hat{Z}_0(kt) e^{-\nu k^2 t^3/3}, \quad (7.11)$$

and equation (7.9) to (4.7). This is Kelvin's (1887) and Orr's (1907) solution of the Couette problem, and can be derived without matched asymptotic expansion. It represents the continuous spectrum of the problem, as pointed out in §4. The solution (7.11) illustrates the essential physics of the linear problem for stable viscous defects. Depending on the form of the initial condition, the factor $\hat{Z}_0(kt)$ can exhibit transient amplification followed by damping. These features reflect inviscid shear dynamics. The viscosity-dependent exponential factor in (7.11) represents a superposed viscous smoothing. Note that this dynamics is associated with a continuous spectrum. In other words, for the defect problem, transient amplification is a property of the continuum, rather than close cancellation of discrete eigenfunctions.

Another special case is provided by the example

$$\hat{f}(q) = \frac{1}{\pi} f e^{s|q|^3} (1 - |q|) H(1 - |q|) \quad (7.12)$$

and

$$\hat{Z}_0(q) = e^{s|q|^3} (Q - |q|) H(Q - |q|), \quad (7.13)$$

where $H(x)$ is the step function, and s and Q are constants. For this profile and initial condition, the two integrals, $\mathscr{D}(ip/k)$ and $\mathscr{N}(p)$, can be evaluated analytically when $\nu/3k = \mu = s$:

$$\mathscr{D}(ip/k) = 1 + \frac{2\rho k^2}{p^3} \left[(2k - p) - (2k + p) e^{-p/k} \right], \quad (7.14)$$

with $\rho = f\mathscr{T}_k$, and

$$\mathscr{N}(p) = \frac{k}{p^2} \left[p - kQ + k\, e^{-pQ/k} \right]. \quad (7.15)$$

Note that $\mathscr{D}(c) = 0$ and (7.14) give an algebraic expression for the spectrum of the defect. With these expressions, the inverse Laplace transform can be evaluated by closing the Bromwich contour in either the left or right half-planes and using Cauchy's residue theorem. If $Q < 1 + kt$, the contour can be closed leftwards, and the integral becomes

$$B = -ik\rho \sum_{j=1}^{\infty} \frac{\mathscr{N}(p_j)}{\mathscr{D}'(ip_j/k)} e^{p_j t}, \quad (7.16)$$

where the p_j are the zeros of $\mathscr{D}(ip/k)$, the normal modes eigenvalues of the defect. If $Q > 1 + kt$, on the other hand, the integral must be split into two parts, one of which closes rightwards and vanishes identically. The remaining piece closes in the

left half-plane leaving

$$B = -\mathrm{i}k^2\rho \sum_{j=1}^{\infty} \frac{p_j - kQ}{p_j^2 \mathscr{D}'(\mathrm{i}p_j/k)} \mathrm{e}^{p_j t} + k^4 \rho Q \frac{\mathscr{D}'(0)}{\mathscr{D}^2(0)} + \frac{3k\rho}{3 - \rho}(1 - kQt), \qquad (7.17)$$

provided $\rho \neq 3$ (which corresponds to a discrete mode with $c = 0$). Hence there is a transient growth of the perturbation until a time $t = (Q - 1)/k$. Thereafter the streamfunction is resolved into the defect normal modes and decays accordingly, unless the profile is unstable.

For general profiles, the calculation of the integrals cannot be done analytically. However, it is straightforward to evaluate them numerically, which may be of use in some applications. Also, it is possible to extract some general criteria that determine whether perturbations grow and how they decay. These details depend on the asymptotic forms of $\mathscr{N}(p)$ and $\mathscr{D}(\mathrm{i}p/k)$ for large $|p|$. Those forms are in turn determined by the behaviour of the Fourier transforms of the profile, $\hat{F}$, and the initial condition, $\hat{Z}_0$. In general, stationary-phase arguments like those of Appendix A indicate that, as the real part of p becomes large and negative,

$$\mathscr{N}(p) \sim \exp(-c_1 |p|^{n/(n-1)}) \quad \text{and} \quad \mathscr{D}(\mathrm{i}p/k) \sim \exp(-c_2 |p|^{m/(m-1)}), \qquad (7.18)$$

for some constants c_1 and c_2, and integers, n and m both greater than 2. (For the examples of §5, $m = 3$, whereas the special cases (7.12) and (7.13) are equivalent to taking $n, m \to \infty$.)

If $t + c_2 |p|^{1/m} > c_1 |p|^{1/n}$, then the Bromwich contour can be closed in the left half-plane for all time. This leads to a streamfunction like (7.16), a sum over the discrete modes of the defect. This presumably corresponds to a circumstance where the perturbation is more localized than the defect. As a result, the perturbation can be represented as a sum over the discrete normal modes of the defect. If $t + c_2 |p|^{1/m} < c_1 |p|^{1/n}$, then the contour cannot be closed in this way, and terms modelling transient amplification may result, as in (7.17).

If we select initial conditions such that $n \to \infty$, then the criterion for closing left becomes $t + c_2 |p|^{1/m} > c_1$. In this situation, we can rearrange (7.8) into

$$B(t) = -\mathscr{T}_k \hat{Z}_0(kt) \mathrm{e}^{-vk^2 t^3/3} - \frac{1}{2\pi \mathrm{i}} \mathscr{T}_k \int_{\mathscr{C}} \mathrm{e}^{pt} \mathscr{N}(p) \frac{1 - \mathscr{D}(\mathrm{i}p/k)}{\mathscr{D}(\mathrm{i}p/k)} \, \mathrm{d}p. \qquad (7.19)$$

Provided that $t > c_1$, we may then close the Bromwich contour in the left half-plane, and the remaining integral reduces, leaving

$$B(t) = -\mathscr{T}_k \hat{Z}_0(kt) \mathrm{e}^{-vk^2 t^3/3} + \mathrm{i}k \mathscr{T}_k \sum_{j=1}^{\infty} \mathrm{e}^{p_j t} \frac{\mathscr{N}(p_j)}{\mathscr{D}'(\mathrm{i}p_j/k)} \, \mathrm{d}p. \qquad (7.20)$$

That is, the streamfunction separates into a contribution from the continuous spectrum like the Couette case, and a sum over the defect normal modes.

8. Closing remarks

To summarize, the defect approximation leads to a tractable reduced equation that contains much of the physics of viscous shear flow. With it, one can derive explicit dispersion relations for the normal modes. These relations facilitate a complete study of the spectrum, and allow one to fashion Nyquist methods to locate and catalogue the various kinds of instabilities. Moreover, with the explicit formulae to hand, it is a

simple matter to analyse the inviscid limit. Then one can identify the features of the shear that lead to viscous destabilization, and connect the limits of viscous eigenmodes with the inviscid instabilities and quasi-modes. Finally, defect theory permits one to open weakly nonlinear expansions and solve the initial-value problem with Laplace transforms. These features should make the defect theory of singular importance in understanding viscous shear flow.

Other avenues that defect theory open are into more complicated flows and fluids. For example, one can consider compressible stratified fluids, magnetohydrodynamic shears and non-Newtonian fluid defects. In the latter example, there are complicated constitutive models that couple to the shear equations, but which are simplified substantially by the defect expansion (Balmforth & Craster 1997). In fact, it is partially these more complicated applications that have motivated the present study.

The main drawback of the defect theory is that it is only two-dimensional. The importance of the third dimension in the turbulent transition of real fluids cannot be overstressed. In some circumstances motion can be constrained to be two-dimensional by, for example, rotation. In those cases, defect theory may capture the dominant physical processes in sheared states. But as a setting in which to explore transition, the theory is sadly insufficient.

Appendix A. The stationary phase calculation

This Appendix describes the stationary phase evaluation of some of the integrals in the main text. To begin, consider the integral

$$\mathscr{J}(z) = \int_0^\infty \mathrm{e}^{-\mu q^3 - \mathrm{i}zq} \, \mathrm{d}q. \tag{A 1}$$

This integral, with $z = -\mathrm{i} - c$ and $\mu = v/3k$, appears in the dispersion relation for the Lorentzian profile (equation (4.1) with $\alpha = 0$ and $\beta = 1$). $\mathscr{J}(z)$ satisfies the differential equation, $3\mu \mathscr{J}'' - \mathrm{i}z\mathscr{J} = -1$, and is also related to the special function $\mathrm{Hi}(z)$ (Abramowitz & Stegun 1972). It has an asymptotic form for large $|z|$ given by

$$\mathscr{J}(z) \sim -\frac{\mathrm{i}}{z} \sum_{n=0}^\infty \frac{(3n)!}{n!} (\mu/\mathrm{i}z^3)^n \quad \text{if} \quad \arg(z) < \frac{\pi}{6} \ \text{or} \ \frac{5\pi}{6} < \arg(z), \tag{A 2}$$

and

$$\mathscr{J}(z) \sim \exp\left(-\tfrac{2}{3}(\mathrm{i}z^3/3\mu)^{1/2}\right) \quad \text{if} \quad \frac{\pi}{6} < \arg(z) < \frac{5\pi}{6}. \tag{A 3}$$

The first of these forms arises from an expansion around the lower limit of the integral, and is obtained by repeated integrations by parts or from consideration of the differential equation; the second is a stationary phase contribution. The lines $\arg(z) = \pi/6$ and $\arg(z) = 5\pi/6$ are the demarcation between the regions in which either (A 2) or (A 3) dominates. In fact, these lines delineate the 'wedge' beside which most of the eigenvalues are distributed for this profile. To capture the asymptotic form of the eigenvalue relation, an expansion near the wedge, containing both (A 2) and (A 3), is needed.

When $\arg(z)$ lies close to $\pi/6$ or $5\pi/6$, the points of stationary phase of the integrand in (A 1) lie at $q_s = \pm(-\mathrm{i}z/3\mu)^{1/2}$. One of these lies to the left of the imaginary axis and makes no contribution to the integral. The other lies in the fourth quadrant. The

integral can then be evaluated asymptotically by deforming the contour of integration down the imaginary axis, then off on the path of steepest descent moving over the appropriate saddle point, $q = q_s$, and then to $q \to \infty$. The two sections of the integration path then provide two contributions to $\mathscr{J}$:

$$\mathscr{J}(z) \simeq -\frac{\mathrm{i}}{z} + \pi^{1/2}(3\mu z)^{-1/4} \exp\left[\frac{\mathrm{i}\pi}{8} - \frac{2}{3}\mathrm{e}^{\mathrm{i}\pi/4}\left(\frac{z^3}{3\mu}\right)^{1/2}\right]. \tag{A 4}$$

Introduction of this asymptotic form into the dispersion relation gives, for $c = -\mathrm{i}+\lambda\mathrm{e}^{\mathrm{i}\varepsilon}$,

$$\lambda^2 - \tfrac{1}{2}\rho - \pi^{1/2}\rho\Gamma^{3/2}\sin\left(\tfrac{2}{3}\Gamma - \frac{5\pi}{12}\right)\mathrm{e}^{(\varepsilon+\pi/2\pm\pi/3)\Gamma} \simeq 0 \tag{A 5}$$

and

$$\frac{\sqrt{3}}{2} - \pi^{1/2}\Gamma^{3/2}\cos\left(\tfrac{2}{3}\Gamma - \frac{5\pi}{12}\right)\mathrm{e}^{(\varepsilon+\pi/2\pm\pi/3)\Gamma} \simeq 0, \tag{A 6}$$

where

$$\Gamma = (\lambda^3/3\mu)^{1/2}. \tag{A 7}$$

Equations (A 5) and (A 6) are derived assuming that $\lambda^3/\mu \geqslant 1$. From these relations it follows that

$$c \simeq -\mathrm{i} + \left[\frac{9\pi^2\mu}{4}\left(n + \frac{11\pi}{12}\right)^2\right]^{1/3}\mathrm{e}^{\mathrm{i}\varepsilon}, \tag{A 8}$$

where

$$\varepsilon = -\frac{\pi}{2} \pm \frac{\pi}{3} + \Gamma^{-1}\log\left[(-1)^n\frac{\pi^{1/2}\rho\mu^{-1/4}\lambda^{1/4}}{(1 - \rho/2\lambda^2)}\right]. \tag{A 9}$$

Equation (A 9) indicates that n is either even or odd depending on the sign of ρ, which leads to the interweaving of the eigenvalues along a common asymptotic curve (see figure 10). The asymptotic curves given by (A 8) and (A 9) are drawn on figure 10(*a*).

If the integral is now modified to

$$\mathscr{J}(c) = \int_0^\infty \mathrm{e}^{-\nu q^3/3k+\mathrm{i}cq-q^2/2}q\,\mathrm{d}q, \tag{A 10}$$

then it is possible to follow the same route to derive the asymptotic form of the dispersion relation for the Gaussian profile. In this case,

$$\mathscr{J} \sim \exp{-c^2/4} \quad \text{if} \quad -3\pi/4 < \arg(c) < -\pi/4, \tag{A 11}$$

and for $\arg(c)$ outside this range, $\mathscr{J}$ has a power series expansion like (A 2). If one ignores the contribution to the integral from the lower limit (which gives the correct eigenvalue scalings), then the dispersion relation is written in the form,

$$1 + \tfrac{1}{4}\mathrm{i}\pi^{1/2}\rho c\mathrm{e}^{-c^2/4} \simeq 0, \tag{A 12}$$

which leads to

$$c \sim -(1 \pm \mathrm{i})[(n + 1/4)\pi]^{1/2}\,\mathrm{e}^{\mathrm{i}\varepsilon}, \tag{A 13}$$

where ε is now given by

$$\varepsilon = \frac{1}{2\pi(n + 1/4)}\log\left[\tfrac{1}{4}(-1)^{n+1}\pi\rho[(n + 1/4)]^{1/2}\right]. \tag{A 14}$$

Finally, the third of the illustrative profiles can be dealt with exactly as for the Lorentzian. The relevant integral is (A 1) with $z = -c$ and $\mu = (1 + v/k)/3$. The same stationary phase calculation leads to (A 5) and (A 6), but now with $c = \lambda e^{i\varepsilon}$ and $\Gamma = [k\lambda^3/(v + k)]^{1/2}$. Hence (5.8) follows.

Appendix B. Weakly nonlinear expansion

This Appendix sketches the derivation of the amplitude equation arising in the vicinity of a stability boundary. At a neutral point, there is a neutral eigenmode with wave speed c; in the weakly nonlinear theory, the amplitude of this mode, A, is assumed to be a function of a longer time scale, $T = \delta^2 t$. Moreover, to break the condition of neutrality, the viscosity is expanded as $v = v_0 + \delta^2 v_2$. The governing equations can then be written as

$$Z_t + \eta Z_x + F'B_x - v_0 Z_{\eta\eta} = -(Z_\eta B_x + \delta^2 Z_T - \delta^2 v_2 Z_{\eta\eta}) \tag{B 1}$$

and

$$B = -\int_{-\infty}^{\infty}\int_{-\infty}^{\infty}\int_{-\infty}^{\infty} \mathscr{T}(k)\, e^{ik(x-x')} Z(x', \eta, t, T)\, d\eta\, dx'\, dk, \tag{B 2}$$

where $\mathscr{T}(k) = \tanh k/2k$. On using the Fourier transform in η, these equations become

$$\hat{Z}_t + i\hat{z}_{xq} + iq\hat{F}B_x + v_0 q^2 \hat{Z} = -(iq\hat{z}B_x + \delta^2 \hat{Z}_T + \delta^2 v_2 q^2 \hat{Z}) \tag{B 3}$$

and

$$B = -2\pi \int_{-\infty}^{\infty}\int_{-\infty}^{\infty} \mathscr{T}(k) e^{ik(x-x')} \hat{Z}(x', 0, t, T)\, dx'\, dk. \tag{B 4}$$

If the asymptotic series, $\hat{Z} = \delta \hat{Z}_1 + \delta^2 \hat{Z}_2 + \delta^3 \hat{Z}_3 + ...$ and $B = \delta B_1 + \delta^2 B_2 + \delta^3 B_3 + ...$, are now substituted into (B 3) then that equation can be divided into relations of like order in δ to give

$$O(\delta): \qquad \hat{Z}_{1t} + i\hat{Z}_{1xq} + iq\hat{F}B_{1x} + v_0 q^2 \hat{Z}_1 = 0, \tag{B 5}$$

$$O(\delta^2): \qquad \hat{Z}_{2t} + i\hat{Z}_{2xq} + iq\hat{F}B_{2x} + v_0 q^2 \hat{Z}_2 = -iq\hat{Z}_1 B_{1x} \tag{B 6}$$

and

$$O(\delta^3): \qquad \hat{Z}_{3t} + i\hat{Z}_{3xq} + iq\hat{F}B_{3x} + v_0 q^2 \hat{Z}_3 = -(iq\hat{Z}_1 B_{2x} + iq\hat{Z}_2 B_{1x} + \hat{Z}_{1T} + v_2 q^2 \hat{Z}_1). \tag{B 7}$$

Also, (B 4) is divided into the three relations of a similar form for each order.

B.1. *Order δ*

Equation (B 5) has solution,

$$\hat{Z}_1 = A(T)\xi(q)\, e^{ik_0(x-ct)} + A^*(T)\bar{\xi}(q)\, e^{-ik_0(x-ct)}, \tag{B 8}$$

where k_0 is the wavenumber and c the wavespeed of the neutral mode, and $\bar{\xi}(q) \equiv \xi^*(-q)$. The eigenfunction ξ is found to satisfy

$$\xi_q - 3\mu q^2 \xi + ic\xi = 2\pi q\hat{F}\mathscr{T}_1 \xi(0), \tag{B 9}$$

where $\mathscr{T}_1 = \mathscr{T}(k_0)$ and $\mu = v_0/3k_0$. At this point of the expansion, (B 8) leaves open the scaling of the overall amplitude of ξ. Hence, without loss of generality, $\xi(0)$ can be taken equal to unity. The marginal eigenfunction is therefore

$$\xi = -2\pi\mathscr{T}_1 e^{\mu q^3 - icq} \int_q^{\infty} \hat{F}(\tilde{q})\, e^{-\mu\tilde{q}^3 + ic\tilde{q}} \tilde{q}\, d\tilde{q} \tag{B 10}$$

and

$$B_1 = -2\pi A \mathscr{T}_1 \mathrm{e}^{\mathrm{i}k_0(x-ct)} + \text{c.c.},\tag{B 11}$$

where c satisfies the dispersion relation (4.5). Note that the solution expressed in (B 9)–(B 11) assumes that there is only a single neutral mode with speed c.

B.2. *Order* δ^2

At second order, the solution can be taken to have the form

$$\hat{Z}_2 = |A|^2 \zeta_0 + A^2 \zeta_2 \mathrm{e}^{2\mathrm{i}k_0(x-ct)} + A^{*2} \bar{\zeta}_2 \mathrm{e}^{-2\mathrm{i}k_0(x-ct)}\tag{B 12}$$

and

$$B_2 = -2\pi \left[|A|^2 \mathscr{T}_0 \zeta_0(0) + A^2 \mathscr{T}_2 \zeta_2(0) \mathrm{e}^{2\mathrm{i}k_0(x-ct)} + A^{*2} \mathscr{T}_2 \bar{\zeta}_2(0) \mathrm{e}^{-2\mathrm{i}k_0(x-ct)} \right],\tag{B 13}$$

where $\mathscr{T}_0 = \mathscr{T}(0)$ and $\mathscr{T}_2 = \mathscr{T}(2k_0)$. The amplitude functions ζ_0 and ζ_2 are given by

$$\zeta_0 = 2\pi \frac{k_0 \mathscr{T}_1}{v_0 q} (\xi - \bar{\xi})\tag{B 14}$$

and

$$\zeta_2 = -2\pi \mathrm{e}^{\mu q^3/2 - \mathrm{i}cq} \int_q^\infty \left[\tfrac{1}{2}\mathscr{T}_1 \xi + \mathscr{T}_2 \hat{F} \zeta_2(0) \right] \mathrm{e}^{-\mu \tilde{q}^3/2 + \mathrm{i}c\tilde{q}} \tilde{q} \, \mathrm{d}\tilde{q},\tag{B 15}$$

with

$$\zeta_2(0) = -\frac{\pi \mathscr{T}_1}{D_2} \int_0^\infty \xi \mathrm{e}^{-\mu q^3/2 + \mathrm{i}cq} q \, \mathrm{d}q\tag{B 16}$$

and

$$D_2 = 1 + 2\pi \mathscr{T}_2 \int_0^\infty \hat{F} \mathrm{e}^{-\mu q^3/2 + \mathrm{i}cq} q \, \mathrm{d}q.\tag{B 17}$$

B.3. *Order* δ^3:

Finally, at third order, the inhomogeneous right-hand side to (B 7) contains terms proportional to $\mathrm{e}^{\mathrm{i}k_0(x-ct)}$. In general, such terms lead to unbounded particular solutions unless one takes the Fredholm alternative, which can be written in the form

$$A_T = \gamma A + \varpi |A|^2 A,\tag{B 18}$$

with

$$\gamma = -\frac{1}{I} \int_0^\infty \xi \, \mathrm{e}^{-\mu q^3 + \mathrm{i}cq} q^2 \mathrm{d}q \equiv \frac{2\pi \mathscr{T}_1}{3I} \int_0^\infty \hat{F} \, \mathrm{e}^{-\mu q^3 + \mathrm{i}cq} q^4 \, \mathrm{d}q,\tag{B 19}$$

$$\varpi = -2\pi \frac{k_0}{I} \int_0^\infty [2\mathscr{T}_2 \zeta_2(0)\bar{\xi} + \mathscr{T}_1 \zeta_0 - \mathscr{T}_1 \zeta_2] \, \mathrm{e}^{-\mu q^3 + \mathrm{i}cq} q \, \mathrm{d}q\tag{B 20}$$

and

$$I = \int_0^\infty \xi \, \mathrm{e}^{-\mu q^3 + \mathrm{i}cq} \, \mathrm{d}q \equiv -2\pi \mathscr{T}_1 \int_0^\infty \hat{F} \, \mathrm{e}^{-\mu q^3 + \mathrm{i}cq} q^2 \, \mathrm{d}q.\tag{B 21}$$

REFERENCES

ABRAMOWITZ, M. & STEGUN, I. A. 1972 *Handbook of Mathematical Functions.* Wiley Interscience.

BALMFORTH, N. J., DEL-CASTILLO-NEGRETE, D. & YOUNG, W. R. 1996 Dynamics of vorticity defects in shear. *J. Fluid Mech.* **333**, 197–230 (referred to herein as paper I).

BALMFORTH, N. J. & CRASTER, R. V. 1997 Dynamics of defects in visco-elastic shear. *J. Non-Newtonian Fluids* **72**, 281–304.

CASE, K. M. 1960 Stability of inviscid plane Couette flow. *Phys. Fluids* **3**, 143–148.

DEL-CASTILLO-NEGRETE, D., YOUNG, W. R. & BALMFORTH, N. J. 1995 Vorticity dynamics in shear flow. In *Proc. 1995 Summer Study Program on Geophysical Fluid Dynamics* (ed. R. Salmon). *Woods Hole Oceanographic Institution Tech. Rep.*

DAVEY, A. 1973 On the stability of plane Couette flow to infinitesimal disturbances. *J. Fluid Mech.* **57**, 369–380.

DRAZIN, P. G. 1961 Discontinuous velocity profiles for the Orr–Sommerfeld equation. *J. Fluid Mech.* **10**, 571–583.

DRAZIN, P. G. & REID, W. H. 1981 *Hydrodynamic Stability*. Cambridge University Press.

GILL, A. E. 1965 A mechanism for instability of plane Couette flow and of Poiseuille flow in a pipe. *J. Fluid Mech.* **21**, 503–511.

HOWARD, L. N. 1959 Hydrodynamic stability of a jet. *J. Maths Phys.* **37**, 283–298.

KELVIN, LORD 1887 Rectilinear motion of fluid between two parallel plates. *Phil. Mag.* **24**, 188–196.

LENARD, A. & BERNSTEIN, I. B. 1958 Plasma oscillations with diffusion in velocity space. *Phys. Rev.* **112**, 1456–1459.

LIN, C. C. 1945 On the stability of two-dimensional parallel flows. *Q. Appl. Maths* **3**, 117–142, 218–234, 277–301.

LIN, C. C. 1955 *The Theory of Hydrodynamic stability*. Cambridge University Press.

MURDOCK, J. W. & STEWARTSON, K. 1977 Spectra of the Orr–Sommerfeld equation. *Phys. Fluids* **20**, 1404–1411.

ORR, W. McF. 1907. The stability of the steady motions of a perfect fluid and of viscous fluid. *Proc. R. Irish Acad.* **27**A, 9–27, 69–138.

PENROSE, O. 1960 Electrostatic instabilities of a uniform non-Maxwellian plasma. *Phys. Fluids* **3**, 258–265.

SCHMID, P. J., HENNINGSON, D. S., KHORRAMI, M. R., & MALIK, M. R. 1993 A study of eigenvalue sensitivity for hydrodynamic stability operators. *Theor. Comput. Fluid Dyn.* **4**, 227–240.

STEWARTSON, K. 1978 The evolution of the critical layer of a Rossby wave. *Geophys. Astrophys. Fluid Dyn.* **9**, 185–200.

STEWARTSON, K. 1981 Marginally stable inviscid flows with critical layers. *IMA J. App. Maths* **27**, 133–175.

STUART, J. T. 1960 On the nonlinear mechanics of wave disturbances in stable and unstable parallel flows. Part 1. The basic behaviour in plane Poiseuille flow. *J. Fluid Mech.* **9**, 353–370.

WARN, T. & WARN, H. 1978 The evolution of a nonlinear critical level. *Stud. Appl. Maths* **59**, 37–71.